Synaptic Actions of Fibroblast Growth Factor -1 in the Hypothalamus and Dorsal Vagal Complex

Brandon L. Roberts[1]*, Sarah R. Lindsley[1], Katherine Tennant[1], Eric Kim[1], and Paul Kievit[1]

[1]Division of Cardiometabolic Health, Oregon National Primate Research Center, Beaverton, OR 97006, USA

INTRODUCTION

The dorsal vagal complex (DVC) and arcuate nucleus of the hypothalamus (ARH) are two central sites that are highly involved in metabolism and food intake [1]. **Two sites in the DVC that are involved in food intake and are glucose-sensitive are the nucleus of the solitary tract (NTS) and area postrema** [2,3].

The NTS is the primary site receiving information from the gut, via vagal afferent inputs, while the area postrema is a circumventricular organ that senses circulating signals, such as blood glucose [4,5]. These sites have reciprocal connections and **the NTS projects extensively throughout the brain, including to the ARH** [6].

The ARH is home to two highly studied subpopulations of neurons, the **anorexigenic** β-endorphin and alpha-melanocyte-stimulating hormone expressing proopiomelanocortin **(POMC) neurons** and **orexigenic neuropeptide Y (NPY) neurons**, which co-express agouti-related peptide (AgRP) [7-9].

Fibroblast growth factor -1 (FGF1) is a mitogen involved in embryonic development and angiogenesis [10,11]. Central and peripheral administration of **FGF1 improves insulin secretion, corrects hyperglycemia, reduces food intake, and induces pERK1/2 and cFos expression** the ARH and median eminence in diabetic rodent models [12,13].

Here we begin to **elucidate the synaptic mechanisms of FGF1 actions on ARH-POMC and -NPY neurons**.

Given that the DVC directly communicates with the ARH and is the primary site directly connecting the brain to the gut, liver and pancreas, we **also explore the effects of FGF1 on neurons in the NTS and area postrema** [1,14-17].

METHODS

Brain Slice Preparation. Coronal slices from POMC-EGFP or NPY-GFP mice were cut to preserve the ARH or DVC. Whole cell recordings were made using an external bath solution containing: (mM) 124 NaCl, 5 KCl, 2.6 NaH_2PO_4, 10 HEPES, 2 $MgSO_4$, 26 $NaHCO_3$, 2 $CaCl_2$, 5 Dextrose and bubbled with 95% O_2 / 5% CO_2 at 30-34 °C; pH=7.3, adjusted to 305-315 mOsm using sucrose. The internal current-clamp and EPSC voltage-clamp recording solution contained (mM): 125 K-Gluconate, 2 KCl, 5 HEPES, 10 EGTA, 5 MgATP, 0.25 NaGTP; the voltage-clamp internal recording solution contained: 140 CsCl, 5 $MgCl_2$, 1 BAPTA, 10 HEPES, 5 MgATP, 0.25 NaGTP, pH=7.3, 295-305 mOsm. Application of TTX, CNQX and AP-5 was used to record mIPSCs and TTX and bicucculine were used to record mEPSCs. Neurons were recorded from the ARH, NTS, or area postrema. Only neurons not exceeding holding currents of 50 pA at V_H= -60 mV for the 10 min control period (input resistance > 120 MΩ) were studied further.

Immunohistochemistry. Cannulas were placed i.c.v. in the third ventricle. Animals were randomized according to body weight and food intake. Mice were dosed i.c.v. (2μl) and sacrificed 90 min post injection. Brains were removed, cryoprotected in 20% sucrose, frozen, and cut at 25 μm. Sections were stained using a polyclonal rabbit anti–c-Fos antibody (1:10,000, SC-52; Santa Cruz Biotechnology), amplified (PK-4000; Vectastain ABC HRP kit), and visualized with nickel-DAB (DAB Kit, SK-4100; Vector Laboratories). Sections were mounted on slides and imaged with an Olympus brightfield slide scanner. c-Fos positive cells were counted by hand using ImageJ software.

Mice. All mice were on a C57Bl/6J background. Mice were 8-16 weeks old at time of cell recordings. DIO mice were placed on a 60% HFD for 12-16 weeks before tissue collection.

Statistics. For recordings, within cell analysis was determined using Kolmogorov-Smirnov test and between cell analysis using a one-way ANOVA or repeated measures mixed-model design. Error bars indicate SEM; *p < 0.05, **p < 0.01 denotes a significant change.

REFERENCES

1. **Berthoud, H.R.,** Neurogastroenterol Motil, 2008. 20 Suppl 1: p. 64-72.
2. **Roberts, B.L., et al.,** Am J Physiol Regul Integr Comp Physiol, 2017. 313(3): p. R229-R239.
3. **Ritter, S., T.T. Dinh, and Y. Zhang,** Brain Res, 2000. 856(1-2): p. 37-47.
4. **Price, C.J., T.D. Hoyda, and A.V. Ferguson,** Neuroscientist, 2008. 14(2): p. 182-94.
5. **Browning, K.N. and R.A. Travagli,** Auton Neurosci, 2011. 161(1-2): p. 6-13.
6. **Ito, H. and M. Seki,** Okajimas Folia Anat Jpn, 1998. 75(1): p. 9-31.
7. **Myers, M.G., Jr. and D.P. Olson,** Nature, 2012. 491(7424): p. 357-63.
8. **Gautron, L., J.K. Elmquist, and K.W. Williams,** Cell, 2015. 161(1): p. 133-145.
9. **Morton, G.J., T.H. Meek, and M.W. Schwartz,** Nat Rev Neurosci, 2014. 15(6): p. 367-78.
10. **Thisse, B. and C. Thisse, Dev Biol,** 2005. 287(2): p. 390-402.
11. **Presta, M., et al.,** Cytokine Growth Factor Rev, 2005. 16(2): p. 159-78.
12. **Brown, J.M., et al.,** Diabetes, 2019. 68(5): p. 1054-1061.
13. **Tennant, K.G., et al.,** Diabetes, 2019. 68(7): p. 1462-1472.
14. **Matsuhisa, M., et al.,** Metabolism, 2000. 49(1): p. 11-6.
15. **Browning, K.N., F.H. Coleman, and R.A. Travagli**, Am J Physiol Gastrointest Liver Physiol, 2005. 288(5): p. G950-5.
16. **Berthoud, H.R. and T.L. Powley**, J Auton Nerv Syst, 1987. 19(1): p. 77-84.
17. **Babic, T., et al.,** J Physiol, 2012. 590(15): p. 3611-22.

RESULTS:

FGF1 depolarizes ARH-POMC neurons

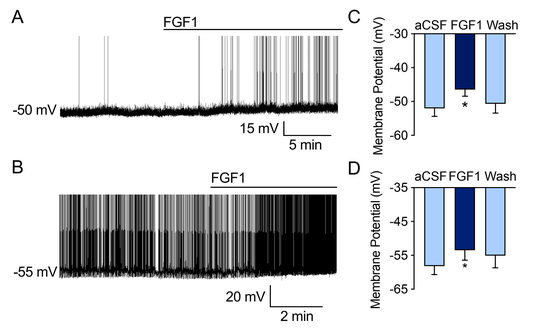

Figure 1. ***A***, Current clamp trace of a ARH-POMC-EGFP neuron from a chow-fed and (***B***) DIO mouse before and after bath application of FGF1 (100 nM). ***C***, Mean membrane in chow-fed (n = 12) and (***D***) DIO mice (n = 13) before and after bath application of FGF1 in ARH-POMC-EGFP neurons.

FGF1 does not alter inhibitory inputs on ARH-POMC neurons

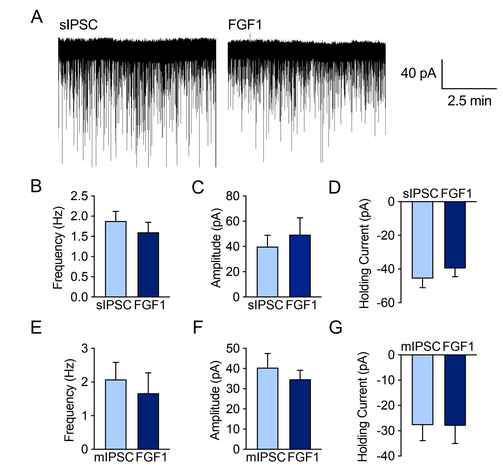

Figure 2. ***A***, Voltage-clamp trace of sIPSC frequency and amplitude after bath application of FGF1 (100 nM) in ARH-POMC-EGFP neurons. ***B***, sIPSC frequency, (***C***) amplitude and (***D***) holding current (n = 11). ***E,*** mIPSC frequency, (***F***) amplitude and (***G***) holding current before and after bath application of FGF1 (n = 9).

FGF1 does not alter excitatory inputs on ARH-POMC neurons

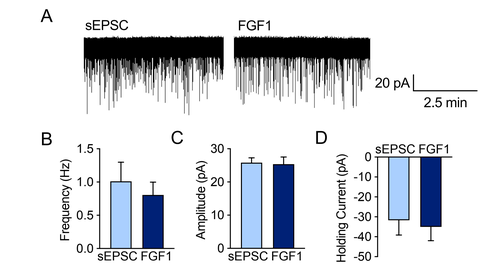

Figure 3. ***A***, Voltage-clamp trace showing no effect of FGF1 (100 nM) bath application on sEPSC frequency in ARH-POMC-EGFP neurons. ***B***, Mean sEPSC frequency, (***C***) amplitude, and (***D***), holding current before and after FGF1 application in ARH-POMC-EGFP neurons (n = 7).

FGF1 actions on ARH-POMC neurons are indirect

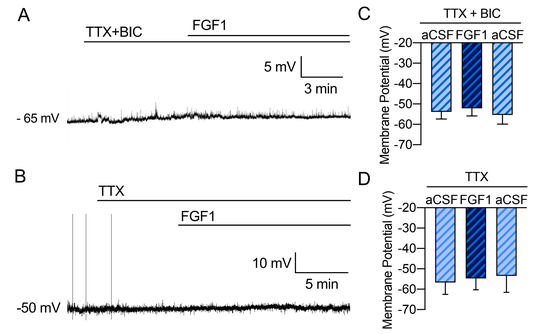

Figure 4. ***A***, Current-clamp trace of a POMC-EGFP neuron after bath application of FGF1 in the presence of TTX + BIC and ***B,*** pretreat with TTX. ***C***, Mean membrane potential after bath application of FGF1 in the presence of TTX +BIC (n = 10) or ***D***, TTX (n = 6).

FGF1 actions on ARH-POMC neurons are independent of FGF receptors

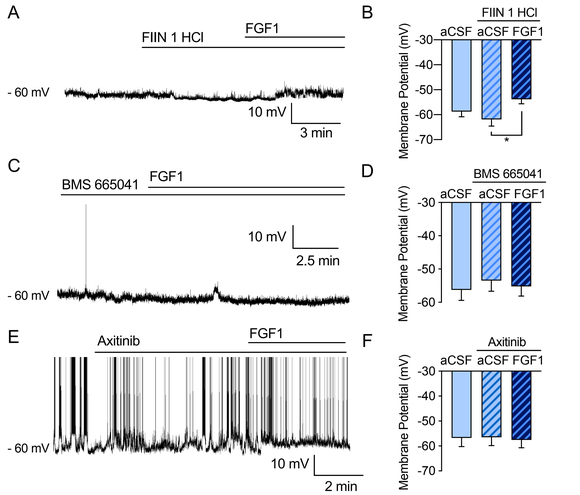

Figure 5. ***A***, Representative trace of a POMC-EGFP neuron after bath application of FGF1 in the presence of FIIN 1 HCl (500 nM) ***B,*** BMS 665041 (1 μM) and ***C***, axitinib (100 nM). ***D,*** Mean membrane potential after bath application of FGF1 in the presence of FIIN HCl (n = 5) ***E,*** BMS 665041(n = 8) or ***F***, axitinib (n = 9)

FGF1 indirectly depolarizes ARH-NPY neurons

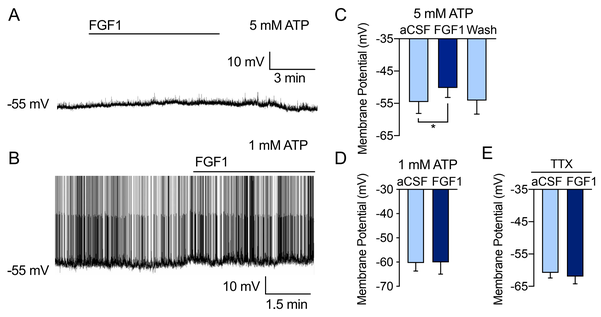

Figure 6. ***A***, Current-clamp trace of a ARH-NPY-GFP neuron from a lean mouse before and after bath application of FGF1 (100 nM) with 5mM and (***B***) 1mM internal ATP concentration. ***C,*** Mean membrane potential before and after bath application of FGF1 with 5mM internal ATP (n = 9) (***D***) and TTX pretreatment (n = 6) or (***E***) with 1mM internal ATP (n = 7).

ICV FGF1 injection induces cFos in the DVC

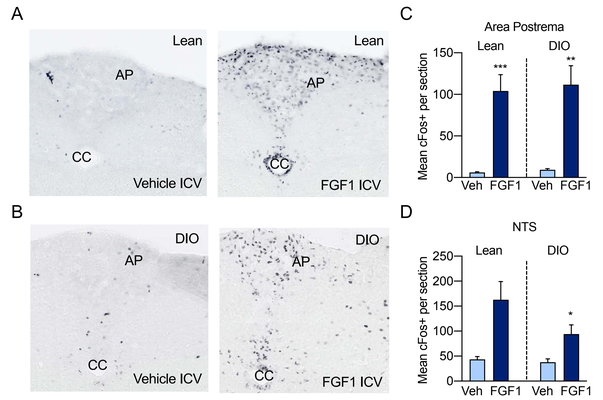

Figure 7. ***A***, Representative images of FGF1 induces cFos activation in the area postrema and NTS of lean and (***B***) DIO mice ***C,*** Mean cFos counts in the area postrema (n = 4-6 mice/group) and (***D***) the NTS of lean and DIO mice (n = 2-3 mice/group)

FGF1 directly depolarizes neurons in the DVC

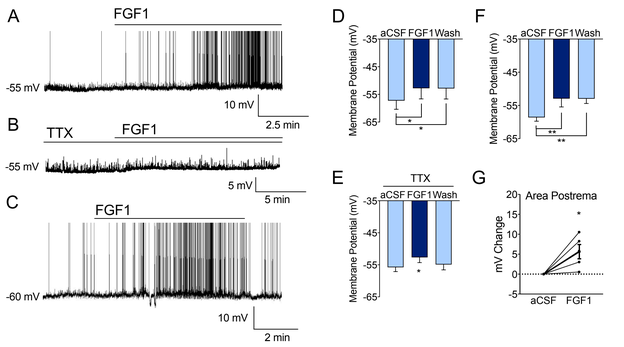

Figure 8. ***A***, Current-clamp trace of a NTS control, (***B***) TTX pretreated, and (***C***) area postrema neuron before and after bath application of FGF1 (100 nM). ***D***, Mean membrane potential before and after bath application of FGF1 in control NTS neurons (n = 10) (***E***) NTS neurons pretreated with TTX (n = 6). (***G***) mV change of area postrema neurons. (n = 5).

SUMMARY

In the Arcuate nucleus of the hypothalamus:

- FGF1 depolarized POMC neurons
- FGF1 effects on POMC and NPY neurons are indirect
- FGF1 effects on POMC neurons are not dependent on FGF receptors

In the dorsal vagal complex:

- FGF1 depolarizes neurons in the area postrema and NTS
- FGF1 has direct actions on neurons in the NTS